Acta Polytechnica CTU Proceedings **38**:228–234, 2022
https://doi.org/10.14311/APP.2022.38.0228

Published by the Czech Technical University in Prague

HYGRIC PERFORMANCE OF NEW BUILDING COMPONENTS FOR VERTICAL GREEN GARDENS

Pavel Kopecký

Czech Technical University in Prague, University Centre for Energy Efficient Buildings, Třinecká 1024, 273 43 Buštěhrad, Czech Republic

correspondence: pavel.kopecky@fsv.cvut.cz

Abstract. The newly developed box-like panel lightweight element for vertical greenery was designed and built at University Centre for Energy Efficient Buildings of the Czech Technical University in 2020. A test site for testing green facade components is operated since spring 2021. Test samples differ in shape, arrangement of functional layers, water distribution means and irrigation patterns. The article presents and discusses measured data at selected test samples during growing season in year 2021. Physical quantities, such as surface temperature of plants, moisture content and matric potential of growing substrate, water inflow and outflow, and ambient boundary conditions, were recorded.

Keywords: Vertical green gardens, real-scale experiment, hygric performance, watering patterns.

1. Introduction

The space next to buildings in urban areas is in particular used for pavements and roads. Solid nonporous materials like concrete and asphalt are used. The built environment lacks green plants if compared with rural areas. Building enclosures can be seen as potential carriers of green plants. Whereas technical solutions for green roofs are established on the market the technical solutions for green vertical walls are still under development. The current state-of-the art of vertical greenery systems is summarized in [1].

Vertical green gardens attached to building walls offer some benefits. Greenery improves the visual quality of built environment, improves soundproofing properties of building enclosures, protects the building enclosure and the internal environment against external climatic loads and may create new ecological niches. Massive usage of green roofs and vertical greeneries within urban areas could mitigate the urban heat island effect [2].

Some disadvantages are however associated with vertical green gardens as well. First, it is known to only limited extent which plants are suitable for given type of climate, environmental conditions of site and the system for vertical greenery. A lack of long-term measurement data from real-scale installations exists. Second, the raw building materials are needed. For instance, some containers to keep growing substrate at place and supporting structures carrying the greenery are needed. Moreover, the irrigation system has to be used in order to compensate for unfavourable environmental conditions at vertical walls. The irrigation system and greenery itself need regular inspections. It can cause non-negligible maintenance costs during operation. It is the subject of current research if some of the disadvantages can be minimized by optimized and reliable technical solutions.

This paper deals with newly developed planar box-like elements for vertical green gardens. Various test samples were built and equipped with measurement sensors in 2021. This article presents a side-by-side comparison of measured hygric performance of several test samples in real climatic conditions of the site located in semi-continental climatic conditions.

2. Materials and methods

2.1. Development of a new technical solution for vertical greenery

The goal was to design a technical solution for vertical greenery which will be suited for vertical walls of industrial buildings (e.g. warehouses and production spaces). The walls of modern industrial buildings are currently being constructed as lightweight sandwich structures with low capacity to carry extra loads. Therefore, it was required that the proposed solution should be lighter than $50\,\mathrm{kg/m^2}$ (i.e. less than half of the system for vertical greenery described in [3]). The requirement of low weight implies the limit on the thickness of soil-type growing substrate ($< 5 \div 6\,\mathrm{cm}$). The soil-type substrate was believed to be applicable for plants under consideration and for semi-continental climatic conditions. Since only one worker should be able to carry the weight of the element, surface area of the element is practically limited to $0.5\,\mathrm{m^2}$.

Water availability is essential for long-term success of plants. The technical solution for vertical greenery must ensure reliable inflow and controlled flow of water through growing substrate leading to uniform and sufficient moisture content. The challenge is to control the vertical redistribution of water due to gravity. The goal is to maintain stable environment with good water availability.

The development of a system for controlled distribution of irrigation water in the element was carried out iteratively by trial and error approach. Several

(a). 26/11/2020. (b). 14/04/2021.

Figure 1. The first prototypes placed on the test façade.

laboratory models of the water distribution system in the characteristic sample were built (06–08/2020). The laboratory experiments tested two conceptual ideas:

(1.) water distribution along the upper edge of the element can be provided by a suitable hydrophilic capillary active material, and

(2.) water distribution in growing substrate can be enhanced by a drainage layer located at the rear side of the panel (behind soil substrate).

Testing of watering concepts finally led to an original solution using a block of hydrophilic mineral wool placed along the top edge of the element. Two parallel plastic plates with teeth shaped bottom edge are pushed in the cut-outs made in the mineral wool. Teeth release drips of water if hydrophilic mineral wool is oversaturated. Water drips into the soil substrate which is enclosed in the honeycomb-like structure of interconnected cells made of recycled plastics (cell size 62.5×62.5 mm, thickness 4 cm). The growing substrate is firmly hold in cells by jute fabric and metal lattice placed on the external side. Water also drips into drainage layer which is located behind growing substrate. The carpet made of recycled polyester was used (thickness 2 cm).

Water moves down through cells with growing substrate and through carpet by means of gravity. The carpet enables faster water transport than soil substrate. The overflow of water from carpet to growing substrate is created in the middle of the height of the element. The carpet is there discontinued by means of horizontal yet sloped cut. The plastic plate with teeth is placed in the cut and sealed to the rear side of the element. Water flow through the carpet is thus diverted from rear side into growing substrate.

The first three test samples (scale 1:2, full height, half width) were built during 09/2020. Two test samples were seed by grass and hanged on the test façade. The test samples were fully green since the end of 10/2020. The test samples were irrigated weekly in the cold period. Grass on both test samples survived cold season in a relatively good shape, albeit showing weaker coverage of the bottom side of both test samples and reduction of leaf area density than in initial state. The fade was mainly associated with one-week long cold period (daily average ambient temperature $< 0\,^{\circ}$C) at beginning of 03/2021. Grass relatively quickly regrown during warmer weeks of spring 2021, even without new seeds (see Figure 1b and Figure 4a, b).

The experience from the cold season showed that capillary redistribution of water in hydrophilic mineral wool does not work reliably. The uniformity of outflow from teeth was dependent on finding the good compromise between total water inflow, size and geometry of mineral wool, and geometry of teeth. Moreover, mineral wool suffered from material degradation and changed its hydraulic properties during the cold season. The distribution of water along the top edge of test samples was therefore redesigned during spring 2021. A thicker plastic pipe with low diameter inlet holes (drilled in angle of 120° and regularly distanced to each other) was placed along the top edge of the sample instead the block of mineral wool. The tests have proven that combination of diameters 13 mm (main pipe) and 1.5 mm (individual outlet holes) leads to uniform outflow of water from holes if water pressure exceeds 2 bars.

Six real-scale test samples were gradually built in 2021. Test samples differed in shape, arrangement of functional layers and water inflow distribution devices. Five samples were hanged on the test façade of the research centre UCEEB. Test sample nr. 4 was built and sent to test site of industrial partner. For differences between samples see Table 1. Main parts of a test sample are depicted in Figure 2. Test samples nr. 3–6 were built in plastic euro containers (size $80 \times 60 \times 12$ cm). Containers for samples nr. 1 and nr. 2 were built from scratch using extruded polystyrene and plywood.

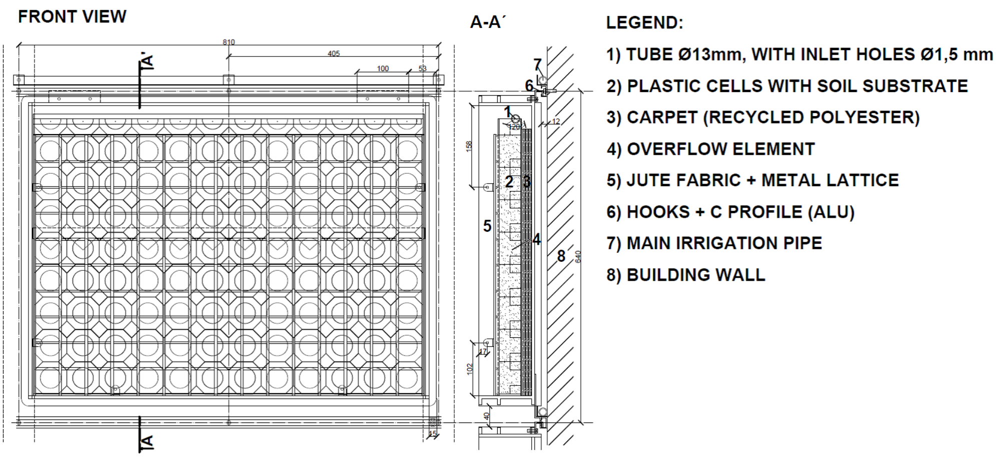

Figure 2. Technical drawing of test sample nr. 3.

Sample	Dimensions	Substrate	Plants	Inflow	Overflow
1	12 × 7 cells (76 × 44 cm)	S1, 43 mm	Grass (standard mixture of seeds)	Block of hydrophilic mineral wool with plastic teeth	Carpet with overflow (4^{th} row)
2	6 × 15 cells (38 × 95 cm)	S1, 43 mm	Grass + Veronica spicata, Rudbeckia hirta	Block of hydrophilic mineral wool with plastic teeth	No carpet
3	12 × 8 cells (76 × 50 cm)	S1, 43 mm	Grass + Veronica spicata, Rudbeckia hirta	Plastic pipe DN 16 mm with capillaries 2 mm	Carpet with overflow (5^{th} row)
5	12 × 8 cells (76 × 50 cm)	S1, 63 mm	Grass + Arabis Alpina, Fragaria Vesca	Plastic pipe DN 13 mm with holes 1.5 mm	No carpet
6	12 × 8 cells (76 × 50 cm)	S2, 63 mm	Thymus serpyllum, Sedum reflexum	Plastic pipe DN 13 mm with holes 1.5 mm	No carpet

S1 – 3 vol. grass substrate / 1 vol. acre substrate.
S2 – 3 vol. grass substrate / 1 vol. acre substrate / 1 vol. sand, 1 vol. expanded clay

Table 1. Definition of test samples.

2.2. Description of test site

The test site for green facade components was built at University Centre for Energy Efficient Buildings in Buštěhrad (UCEEB) during spring 2021. The test site is located on south-east oriented window sill of the experimental curtain wall (at the ground level). The space behind test façade is unheated and ventilated by outdoor air.

The following sensors were used to monitor conditions in test samples:

(1.) temperature sensors (Pt1000, accuracy ± 0.15 K),

(2.) FDR volumetric moisture content sensors (analog Truebner SMT 50 and digital SMT 100, accuracy ± 3 % VWC, no laboratory tests were performed for calibration prior measurement campaign),

(3.) gypsum blocks for measurement of soil water potential (Delmhorst GB2, measuring range −0.1 bar to −15 bar),

(4.) non-contact temperature sensors (infrared radiometers, Apogee SI 421-SS). The boundary conditions were measured on the test facade by EMS 33H, temperature and relative humidity sensor shielded against radiation, accuracy ± 0.15 K, ± 2 % RH. Global solar radiation was measured by EMS11, low cost global radiation sensor. Global radiation data recorded at roof of the research centre were also available. Outflow from test samples 1 and 2 is measured by rain gauge (Pronamic Pro). Positions of sensors are shown in Figure 3.

2.3. Description of irrigation system

The test site was equipped by an automatic irrigation system. The system was used for watering of test samples nr. 1 and nr. 2. The system consists of magnetic valves, balancing valves, water flow meters, compressor, fittings and plastic pipes for water supply to the test facade. The magnetic valves and compressor are both controlled by programmable logic controller (PLC). The compressor enables emptying of the system during cold season in order to prevent damage of external pipes and fittings by water freezing. The logic of the controller can be programmed and tested in Matlab/Simulink environment [4]. The code is then built and run in PLC. Two standard control schemes were used at first:

(a) timer with specification of time and water amount for watering pulse (used in test sample nr. 2) and

(b) feedback control with irrigation controlled according to actual measured moisture content.

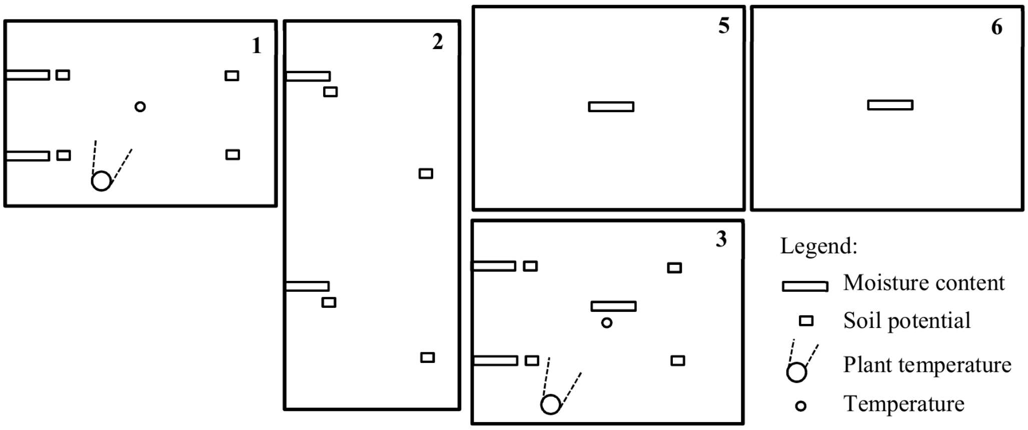

Figure 3. Position of sensors in test samples (external view on test samples – since 08/2021).

Feedback control was used in test sample nr. 1. Test sample nr. 2 used time controller scheme. Morning and evening watering event were usually used in the very warm days. Watering event was constituted by two consecutive pulses. The first watering pulse was used to saturate the upper part of the sample. The second watering pulse transported water from the oversaturated top to the bottom part of the sample. Test samples nr. 3–6 were irrigated by standard commercially available garden timers.

2.4. A method used for estimation of real evapotranspiration

The steady-state thermal balance of the plant surface was used to estimate the real daily evapotranspiration ET from a test sample. The following equation can be derived:

$$ET = \frac{1}{l_v}\left(\alpha_{sol}G_{Gt} - h_{re}(T_{ae} - T_{re}) - \Delta T\left(h_{se} + \frac{1}{R}\right)\right) \quad [\mathrm{kg/(m^2day)}], \tag{1}$$

where

h_{se} [W/(m^{2}K)] is total heat transfer coefficient at plant surface,

h_{re} [W/(m^{2}K)] is radiative heat transfer coefficient at plant surface,

R [m^{2}K/W] is thermal resistance between plant surface and ventilated air gap behind a test sample,

α_{sol} [-] is absorptivity of plants for short-wave radiation,

G_{Gt} [W/m^2] is daily mean global solar irradiance on the test facade,

T_{re} [°C] is daily mean radiant temperature of surrounding surfaces,

l_v [J/kg] is latent hat of water evaporation (2.5×106 J/kg), and

ΔT [K] is the difference between daily mean plant surface temperature T_{pe} and daily mean ambient air temperature T_{ae} ($\Delta T = T_{pe} - T_{ae}$).

For practical calculation, it is assumed that mean radiant temperature is approximately equal to apparent sky temperature ($T_{re} \approx T_{sky}$). The apparent sky temperature is estimated according to [5].

Real evapotranspiration can be alternatively estimated by method [6] as:

$$ET = K_c ET_0 \ [\mathrm{kg/(m^2day)}], \tag{2}$$

where

ET_0 is reference evapotranspiration, i.e. evapotranspiration from grass surface having fixed crop height, surface resistance and albedo, and

K_c is real crop coefficient (time variable).

3. Results

3.1. Visual investigation of test samples

The test façade was visited almost every week during warm season 2021. A diary with impressions and comments was written. Photographs were regularly taken by a mobile phone and by outdoor camera mounted on the stand in front of the façade. Surface patterns recognizable on test samples shows the condition of plants and to some extent moisture content of soil substrate. Figure 4 shows selected days in time period 06–09/2021.

The visual appearance of test samples in June was promising with nice green colour and no brown coloured spots (see Figure 4a). Only the half-size test samples built in 2020 shows lower leaf area density at the bottom part but this is believed to be the consequence of spring freezing week. The figure photographed in July already shows some signs of fade at some locations of test samples (see Figure 4b). There is a brown spot on the right side of test sample nr. 1 and brown area located at the bottom edge of test sample nr. 3. One month later almost all grass of test sample nr. 1 died (see Figure 4c). In September, test sample nr. 1 shows improvement at the bottom and top edge whereas middle part remains brown. Brown spots are evident at test samples nr. 2 and nr. 3 in August and September 2021 (see Figure 4c and d).

(a). 14/06/2021.

(b). 19/07/2021.

(c). 10/08/2021.

(d). 07/09/2021.

Figure 4. Photographs of test façade – selected days in growing season 2021.

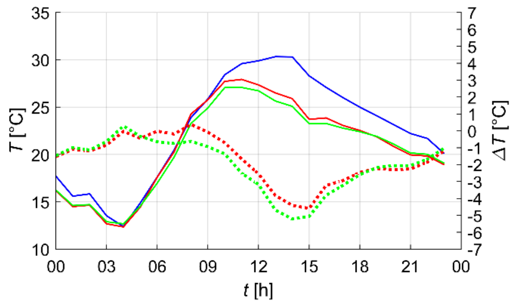

(a). 04/06/2021.

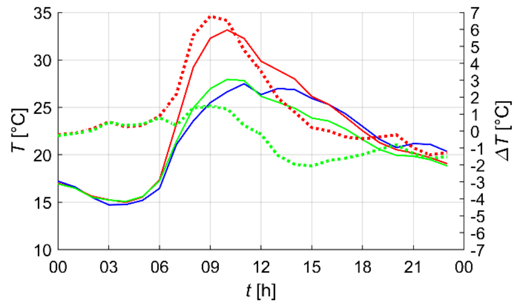

(b). 12/08/2021.

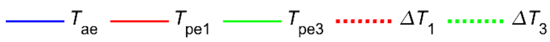

Figure 5. Surface temperature of plants T_{pe} compared with ambient air temperature T_{ae} in two selected clear sky days.

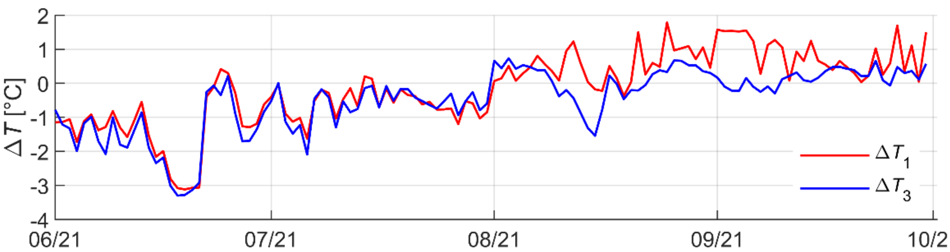

Figure 6. Difference of daily mean plant surface temperature and ambient air temperature (6–9/2021).

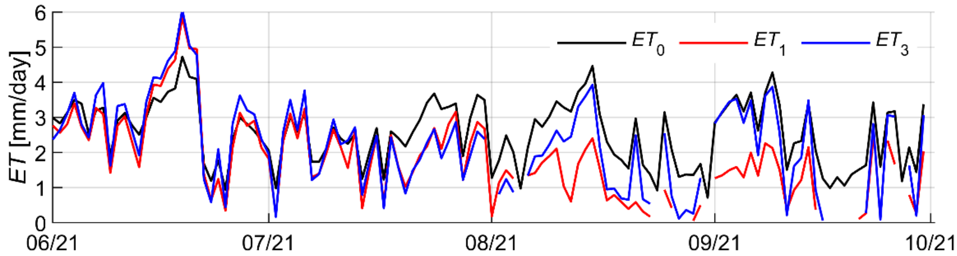

Figure 7. Evapotranspiration of test samples compared with reference evapotranspiration.

Visual observation also showed signs that soil substrate contained excessive amount of water, i.e. brightness of the surface, extrusion of water when soil surface was pressed by fingers, muddy fingers after wiping, and frequent water leaks at the bottom edge of test samples. Mould growth was observed on the jute fabric of test sample nr. 1.

The difference of plant patterns between test samples nr. 3 and nr. 5 deserves comments (see Figure 4c and d). Seeds germinated more quickly on the upper (and moister) part of sample nr. 5, whereas grass grew better at the bottom (and not so moist) part of test sample nr. 5 (see Figure 4, compare c and d). The upper part of test sample is moister since no overflow element was used in test sample nr. 5. Test sample nr. 3 seemingly shows the opposite to test sample nr. 5. Seeds germinated more quickly on the bottom part whereas grass grew well along the upper edge. In this case, the moister part is located at the bottom. The wetness of the bottom part of test sample was caused by the drainage carpet and overflow element used in test sample nr. 3.

3.2. The surface temperature of plants

The measured surface temperature of plants was compared with ambient air temperature in two similar clear sky warm days of growing season (04/07, 12/08). The surface temperature of plants was lower than ambient air temperature by about 4 °C for both test samples in 04/07 (see Figure 5a). The surface temperature of test sample nr. 1 exceeded ambient air temperature by 7 °C in 12/08 whereas test sample nr. 3 maintained undercooling of the plant surface (see Figure 5b). The evolution of the difference between daily mean plant temperature and daily mean ambient air temperature is depicted in Figure 6.

3.3. Daily evapotranspiration

Daily evapotranspiration calculated by Equation 1 is compared with reference evapotranspiration ET_0 in Figure 7.

4. Discussion

The locations with poor plants were documented by photographs (rise of characteristic brown spots visible in photographs). Dying of plants occurred during the second half of growing season and should not be attributed with the lack of available water in root area in this case. In fact, the reason for dying of plants was probably opposite – long term excessively high moisture content of growing substrate. The excess water in root area caused the lack of oxygen in growing substrate.

When one would like to improve the whole concept, operation of irrigation, technical concept and selection of plants would have to be better balanced for given environmental conditions. The task is difficult due to many design variables coming into consideration, e.g. the geometry of cells, position of protruding holes amongst cells, hydraulic properties, thickness and composition of soil substrate, distance between the upper distribution pipe and the bottom edge of the greenery element, position and presence of the overflow elements, amount of water and watering patterns.

5. Conclusions

This study dealt with hygric performance of the newly developed building component for vertical greenery. Investigations were based on measured data and regular visual observations of real-scale test samples in warm season of year 2021. The initial promising growth of plants was replaced by their gradual decline in the second half of growing season. Overwatering is considered to be the main reason for decline of plants.

The presented technical solution of the panel element should be therefore further optimized to obtain better environmental conditions for plants. The main design issue is to find trade-off setting between water storage and water transport properties of the element, i.e. to balance the composition of growing substrate, the shape of plastic cells, position of overflow elements and daily watering patterns. Last but not least it is evident that better understanding of plants would be helpful.

Systematic overwatering showed that watering needs of plants should be better predicted. Therefore, an algorithm for prediction of daily watering needs was programmed in [4] and embedded in PLC. Weather forecast APIs [7, 8] provide access to data for environmental boundary conditions on site in the upcoming day or days. The first test runs were performed at the end of year 2021. The algorithm will be further tested in year 2022.

The test period was limited to growing period of year 2021. The performance of test samples in non-growing period must be studied carefully in continental climatic conditions as well. From practical perspective, it is questionable how to protect pipes and fittings against freeze-thaw damage.

Acknowledgements

This work has been supported by project TAČR TH 03030230. The author is very grateful to Radim Havlíček for his technical assistance.

References

[1] G. Pérez, J. Coma, I. Martorell, L. F. Cabeza. Vertical Greenery Systems (VGS) for energy saving in buildings: A review. *Renewable and Sustainable Energy Reviews* **39**:139–165, 2014. https://doi.org/10.1016/j.rser.2014.07.055

[2] M. Santamouris. Cooling the cities – A review of reflective and green roof mitigation technologies to fight heat island and improve comfort in urban environments. *Solar Energy* **103**:682–703, 2014. https://doi.org/10.1016/j.solener.2012.07.003

[3] P. Kopecký, J. Tywoniak, K. Staněk. Experimental investigation of green façade components for industrial and storage buildings. *IOP Conference Series: Earth and Environmental Science* **588**(5):052049, 2020. https://doi.org/10.1088/1755-1315/588/5/052049

[4] MATLAB, 2020. 9.9.0.1718557 (R2020b), Natick, Massachusetts: The MathWorks Inc.

[5] M. Aubinet. Longwave sky radiation parametrizations. *Solar Energy* **53**(2):147–154, 1994. https://doi.org/10.1016/0038-092X(94)90475-8

[6] R. G. Allen, L. S. Pereira, D. Raes, M. Smith. Crop evapotranspiration – Guidelines for computing crop water requirements – FAO irrigation and drinage paper 56. [2022-01-20]. https://www.fao.org/3/X0490E/x0490e00.htm#Contents

[7] Weather forecast API. [2022-01-20]. https://wp2.pvforecast.cz/

[8] Weather forecast API. [2022-01-20]. https://openweathermap.org/